

## Research Article

# Analysis of Sunshine Temperature Field of Steel Box Girder Based on Monitoring Data

Hailin Lu,<sup>1</sup> Jing Hao ,<sup>1</sup> Jiwei Zhong,<sup>2,3</sup> Yafei Wang,<sup>2,3</sup> and Hongyin Yang <sup>1</sup>

<sup>1</sup>School of Civil Engineering and Architecture, Wuhan Institute of Technology, Wuhan 430074, China

<sup>2</sup>China Railway Bridge Science Research Institute Ltd., Wuhan 430034, China

<sup>3</sup>State Key Laboratory for Health and Safety of Bridge Structures, Wuhan 430034, China

Correspondence should be addressed to Hongyin Yang; yanghongyin02@163.com

Received 18 July 2019; Revised 3 December 2019; Accepted 28 December 2019; Published 30 January 2020

Academic Editor: Valeria Vignali

Copyright © 2020 Hailin Lu et al. This is an open access article distributed under the Creative Commons Attribution License, which permits unrestricted use, distribution, and reproduction in any medium, provided the original work is properly cited.

In this study, based on the recorded meteorological data of the bridge site, a spatial-temporal temperature model of a 3-span steel box girder is developed through applying the thermal analysis software TAITHERM. Firstly, the rationality and dependability of the proposed spatial-temporal temperature model are adequately verified by means of implementing the comparison with the measurement data. Then the temperature distribution of the steel box girder is analyzed and discussed in detail. The analytical results show that the time of the bottom of pavement reaching the daily maximum temperature lags behind the top of pavement by 2 or 3 hours due to the thermal insulation effect of pavement, and the maximum vertical temperature gradient of the structure exceeds the existing standards. Moreover, with the help of the analytical model, a parametric study of comprehensively meteorological factors is also performed. The results of the sensitivity analysis indicate that solar radiation is the most significant factor affecting the maximum vertical temperature gradient of the steel box girder, followed by air temperature and wind speed. After that, with the representative values of the extreme meteorological parameters during 100-year return period in Wuhan City in China being considered as the thermal boundary conditions, the temperature distribution of the steel box girder is further studied for investigation purpose. The results demonstrate that the heat conduction process of the steel box girder has distinct “box-room effect,” and it is of great necessity to consider both the actual weather conditions at the bridge site and the “box-room effect” of steel box girder when calculating thermal behaviors of bridge structures. Finally, it is related that the particular method proposed in this paper possesses a satisfactory application prospect for temperature field analysis upon various types of bridges in different regions.

## 1. Introduction

Studies have shown that steel box girder can successfully combine the advantages of steel and box section girder, including less weight, faster construction speed, and higher flexural and torsional rigidity, which brings tremendous economic benefits to bridge construction. Therefore, the theory and technical research in terms of steel box girder received extensive attention from both the engineering and academia communities. Steel box girder has generally become the most preferred choice for bridges with small and medium spans in recent years [1]. However, the high thermal conductivity and sensitivity to temperature changes of steel may result in the temperature stress of steel box girder

reaching or even exceeding the stress caused by the constant dead load and live load during normal use in some cases [2–4]. In addition, the thermal behaviors of steel structures exposed to natural environments are both significant and complicated, and the temperature distributions in steel bridges are nonlinear in the sunshine [5]. Accordingly, sunshine temperature action is one of the most considerable factors affecting the life-span performance of steel box girders. Thus, to evaluate the temperature effect of bridges accurately, the appropriate temperature distributions must be determined first [6].

For that, considerable efforts have been devoted to studying the temperature distributions on bridges. In general, current research methods can be divided into

mainly two categories, say the theoretical analysis and field measurements. Specifically, the theoretical analysis method is built on the prediction models of temperature field mainly based on the basic principles of heat transfer. In the early 1960s, Zuk [7] and Au et al. [8] investigated the temperature effects on highway bridges by one-dimensional heat transfer theory and pointed out that the temperature variation at the vertical bridge direction was important and complicated. Elbadry and Ghali [9] and Gu et al. [10] studied the influence mechanism of different factors on the temperature field through a series of two-dimensional transient finite element analyses. Kim et al. [11] and Meng and Zhu [12, 13] presented the accurate description of the temperature field through three-dimensional models based on the heat transfer equations, with the application of a bridge as a case study. On the other hand, as for the field measurements method, in addition to the analysis of measurements data directly, the statistical correlation method can also be used to obtain the prediction models. Lee and Kalkan [14] and Liu et al. [15] proposed the temperature gradient patterns that can be utilized to evaluate the effect of thermal gradients by experimental analysis. Ding et al. [16] and Ding and Wang [17] estimated the extreme temperature differences in steel box girder based on long-term measurement data collected by means of the structural health monitoring system employing the extreme value analysis. Hirst [18], Ho and Liu [19], and Lucas et al. [20] analyzed the extreme thermal loadings covering the typical climatic regimes on the basis of the parameter records from the weather bureau by adopting the statistical analysis methodology, which can be used to calculate further extreme temperature gradients.

By comparing the above two categories of research methods, it can be recognized that although the theoretical analysis methods are widely used, the thermal boundary conditions are simplified as the energy equations acting on the numerical models, resulting in the difficulty in obtaining the relatively accurate results. On the other hand, field measurements usually consume large manpower and material resources. Even if the measured data are close to the actual situation, the limitations of the number of measuring points and the testing period make it infeasible to measure the extreme temperature. In addition, although many worldwide studies on the extreme temperature distribution patterns based on measurement data have been conducted, there still exists significant discrepancy among the conclusions. Thus, their application is limited to studying bridges with similar construction and climate conditions. It is concluded that there remain certain problems to be solved for their better application in engineering practices.

As is known to all that China has a vast territory and the climate is rather changeable in different latitudes, in contrast, the uniform standard regulation related to the temperature effect recommended by the General Code for Design of Highway Bridges and Culverts (JTG D60-2015) [21] is likewise not appropriate for each region. For this reason, there is an urgent request to develop the

study on temperature field for bridge structures according to the local meteorological conditions more reasonably. In the present study, a detailed spatial-temporal model of a 3-span curved steel box girder in Wuhan City in the sunshine based on meteorological data is developed, applying the thermal analysis software TAITHERM. After the validation of the model with the monitoring temperature data, the temperature distribution law under the extreme meteorological conditions during 100-year return period is thoroughly analyzed. The investigated results show that the special method proposed in this work can be further applied to study the temperature behaviors of different types of bridges in diverse areas.

## 2. Field Monitoring

*2.1. Engineering Case.* The steel box girder is adopted in this bridge, with a span arrangement of 35 m + 45 m + 35 m, which is shown in Figure 1. The orientation of slightly curved viaduct axis with a curvature radius of 520 m is along the north-south direction. The bridge is located in Wuhan City, China, of which longitude, latitude, and altitude are 114.05°E, 30.07°N, and 23.6 m, respectively. The superstructure is made of a twin-celled single steel box girder with T-shaped stiffeners, and the depth of the girder varies from 2 m at the pier supports to 1.5 m at mid-span in polylines. The steel box girder is made of Q345C steel with a roof width of 10 m and a cantilever width of 2.5 m at both ends. The 10 cm thick high-performance concrete is laid above the roof of the steel box girder, and the 9 cm thick asphalt concrete is used for the pavement, respectively.

According to [22, 23], the temperature differences along the longitudinal direction of a bridge are generally neglected. To monitor the temperature distribution of the box girder in real time, the temperature sensors are laid out on section 1-1 of the side span mid-section. The temperature sensors T1-T11 (LTM8877) are arranged in the girder structure, and the infrared temperature sensor IT1 (IRTP300L) is capable of testing the surface temperature of the pavement; the sensors' distributions are presented in Figure 2. In addition, the temperature data are recorded every 10 minutes.

*2.2. Analysis of Monitoring Results.* The temperature monitoring data of the bridge in September 2018 are analyzed for illustrative purpose. Due to the sunshine, the daily maximum temperature difference of the measured point IT1 of pavement surface is 28°C, which is much larger than the daily temperature difference of 12°C at the other measured points. The comparisons of air temperature, measured temperature of pavement surface, and average temperature of the 11 measuring points of girder are presented in detail in Figure 3. It can be clearly seen that the temperature variation trends of the three are basically the same, whereas there are some remarkable differences in extreme values. To be specific, these minimum values are relatively close, but the maximum temperature of pavement surface is much greater than the average temperature of girder and air temperature,

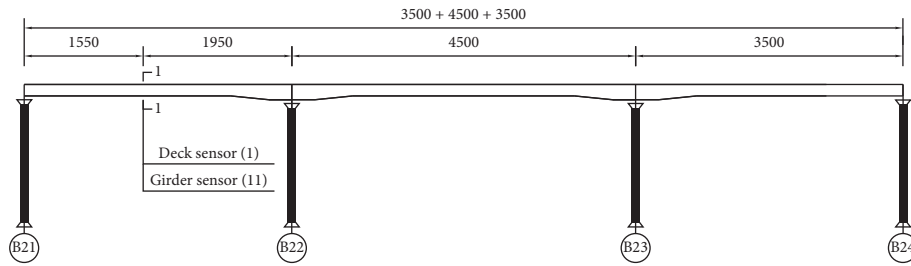


FIGURE 1: Bridge elevation (unit: cm).

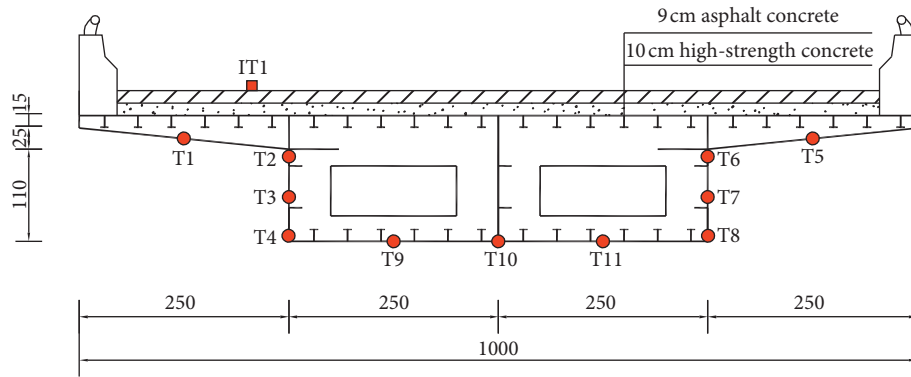


FIGURE 2: Layout of thermal measuring points (unit: cm).

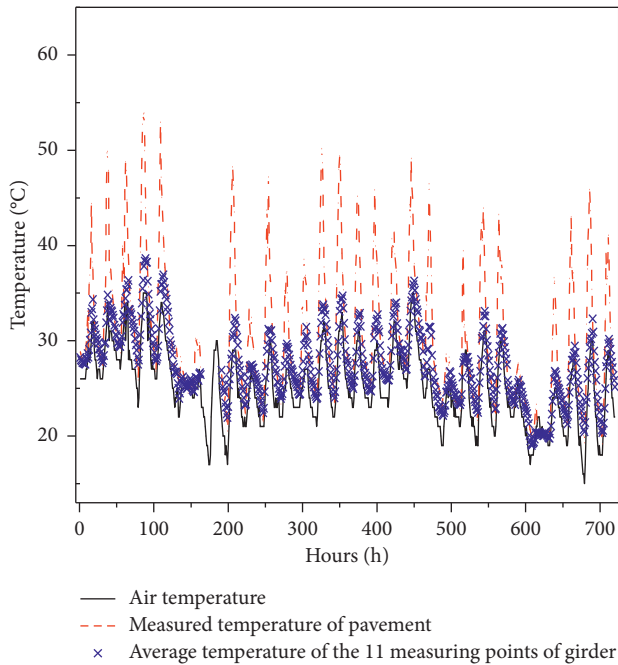


FIGURE 3: Comparisons of air temperature and measured temperature in September.

which indicates that there is an obvious difference of vertical temperature in the section. In fact, the vertical temperature difference refers to that along the vertical direction including pavement, that is, Tem1–Tem3. As shown in Figure 4, Tem3 is the minimum temperature along the vertical direction of the box girder. The monitoring results reveal that the

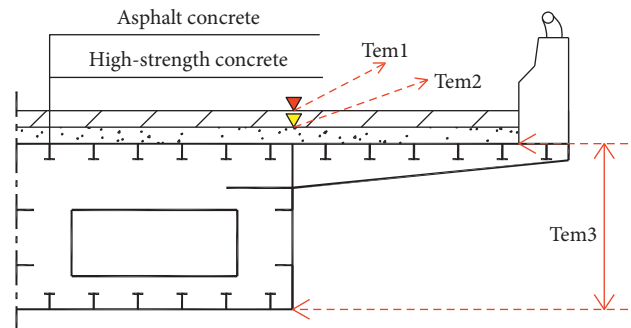


FIGURE 4: Positions of the temperatures.

maximum vertical positive temperature difference usually occurs around 2:00 pm, and its maximum value (18.9°C) appeared at 2:00 pm on September 8th. Moreover, the daily maximum vertical negative temperature difference generally occurs around 5:00 am, and its absolute value is small, generally less than 5°C.

Generally speaking, the bridge design code resists the temperature effect by specifying an extreme temperature gradient. However, the code states that the vertical temperature gradient is just calculated from the bottom of pavement, excluding the pavement, that is, Tem2–Tem3, in Figure 4. Since it is extremely hard to measure the temperature of the bottom of pavement and the thermal conductivity of the materials is different, it is very challenging to determine the temperature of the bottom of the pavement accurately. As a result, it is necessary to develop a reliable calculation model to accurately analyze the temperature field of the steel box girder.

### 3. Spatial-Temporal Simulation of Sunshine Temperature Field of Steel Box Girder

**3.1. Theory of Heat Transfer in Bridge Structure.** As a point of fact, it is the surrounding environment of the bridge structure that determines the structure is always in a three-dimensional unsteady temperature field. The heat exchange process between the steel box girder and the surrounding environment in the sunshine is described in Figure 5. Commonly, the analysis of the temperature field of bridge structure in the sunshine not only involves civil engineering knowledge but also relates to the basic theory of heat transfer, so it is a typical interdisciplinary problem in essence. The temperature at any point in the structure in the natural environment is a function of time and space, and the heat conduction equation in the Cartesian coordinate system is expressed as follows:

$$\rho c \frac{\partial T}{\partial t} = \lambda \left( \frac{\partial^2 T}{\partial x^2} + \frac{\partial^2 T}{\partial y^2} + \frac{\partial^2 T}{\partial z^2} \right) + q, \quad (1)$$

where  $\rho$  and  $c$  denote the density and specific heat of material, respectively,  $\lambda$  is thermal conductivity of objects, and  $q$  denotes heat source intensity in an object.

In theory, it is generally considered that the initial temperature distribution is uniform; namely,  $T(x, y, z, 0) = T_0$  when  $t = 0$ . In engineering practices, the commonly used boundary conditions are involved in equation (2), which are the known functions of the temperature and the heat flux of the structure surface as time changes, respectively. However, it is extremely difficult to solve the analytical solution of temperature field by differential equations for practical bridge engineering. Consequently, the finite element method has become an effective way to obtain the numerical solution and has been widely used [10]:

$$\begin{aligned} T(t) &= f(t), \\ -\lambda \frac{\partial T}{\partial n} &= f(t). \end{aligned} \quad (2)$$

Presently, the thermal analysis software TAITHERM can effectively simulate the three basic heat transfer modes, say the heat conduction, heat convection, and thermal radiation, respectively. Besides, it also has multilevel heat transfer simulation mode and convenient heat conduction modeling mode, and the multiple reflections of heat radiation can be fully considered. Moreover, since TAITHERM can simulate the effects of solar trajectory, cloud occlusion, and scattering by importing hourly meteorological data documents including temperature, radiation, wind speed, humidity, cloud coverage, long-wave radiation, wind direction, rainfall, and other meteorological parameters, it is ideally suitable for long-term transient thermal analysis. At the same time, for the purpose of effectively analyzing the temperature field through applying simulation methodologies, the boundary conditions should be accurately enough. Consequently, the measured meteorological data at the structure site are taken as boundary conditions, resulting in the thermal environment being able to be simulated preferably and veritably. The

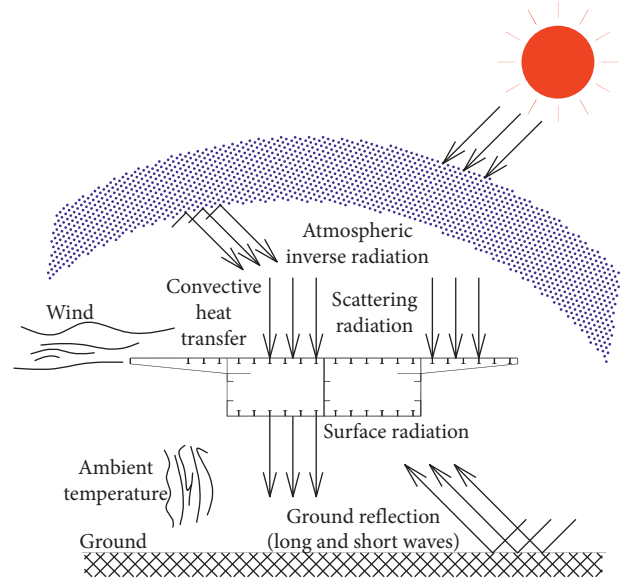


FIGURE 5: Heat exchange process between steel box girder and environment.

input measured meteorological data were collected from local weather stations, which can be downloaded from the WolframAlpha website by directly entering weather, the corresponding city name, and specific date. The hourly meteorological data of the target location can also be obtained from the WolframAlpha website, and it can be conveniently input in TAITHERM as a boundary condition.

Accordingly, taking the meteorological parameters of Wuhan as the thermal boundary conditions, a spatial-temporal temperature field model of the above steel box girder is effectively established by TAITHERM. As a result, the temperature distribution of the steel box girder can be readily calculated by transient analysis.

**3.2. Establishment and Verification of the Developed Spatial-Temporal Model.** A spatial-temporal model of temperature field of the steel box girder is established by taking the hourly meteorological data at the bridge site in September, 2018. Table 1 displays the thermophysical parameters of the materials in the model. For the sake of maintaining the calculation accuracy and efficiency of the model, the steel box girder is further divided into 33 parts, and each part is divided into six layers (the first layer of the top plate part is 9 cm thick asphalt concrete, the second layer is 10 cm thick high-strength concrete, and the remaining four layers are 6 mm thick Q345C steel plate; the other parts are divided into 6 layers of equal-thickness Q345C steel plate). There are in total 135033 elements of the whole model. Although the test period of temperature data is 10 minutes, it was found that the temperature changed a little within 1 hour [24]. Therefore, the time step of the model is set as 1 hour to improve the calculation efficiency. The local schematic diagram of the model is presented in Figure 6.

In order to further improve the accuracy, the above model is modified according to the temperature

TABLE 1: Thermophysical parameters of the materials.

Parameters	Asphalt concrete	Concrete	Q345C steel	Painting <sup>a</sup>
Density (kg/m <sup>3</sup> )	2100	2300	7850	—
Specific heat (J/kg·°C)	886	1010	480	—
Conductivity (W/m·°C)	1.17	0.98	48	—
Absorptivity	0.93	—	—	0.28
Emissivity	0.93	—	—	0.87
Heat coefficient	—	7	5	—

<sup>a</sup>The absorptivity of radiation on the surface of steel box girder is related to the color of the coating, and the bridge surface is painted in white.

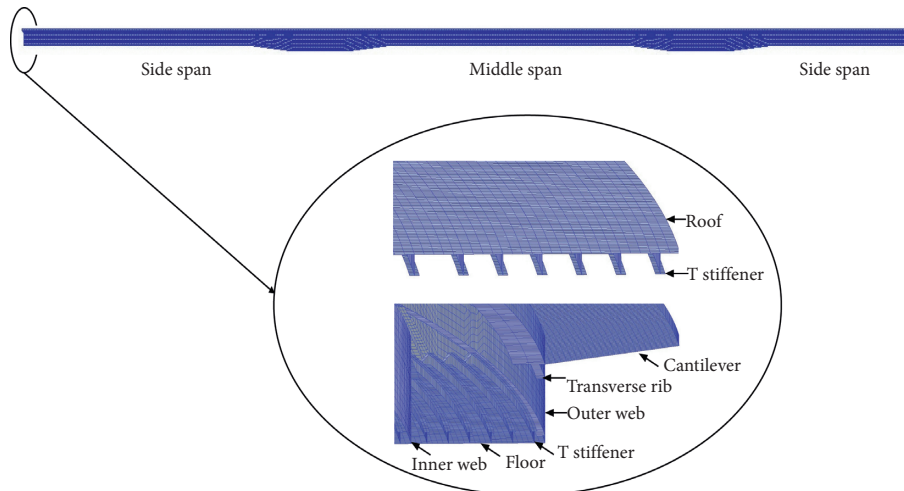


FIGURE 6: Schematic diagram of the model.

monitoring data of the real bridge. However, owing to the limitation of the space, merely the comparisons between calculated and monitored values of typical measuring points are addressed, which are emerged in Figure 7. By careful inspection of the figure, it can be obviously seen that the calculated values of temperature at each measuring point all coincide perfectly with the monitored values, and the variation trends upon the two are consistent. It has been calculated that the errors of the measuring points T1, T3, T10, and IT1 at the flange, web, bottom, and bridge deck are 5.12%, 6.4%, 5.97%, and 7.58%, respectively, which are technically acceptable. It thus fully verifies that the suggested spatial-temporal model of temperature field upon the steel box girder is of superior rationality and applicability. As a result, it can be applied for the accurate analysis of sunshine temperature field of the steel box girder.

**3.3. Analysis of Calculation Results.** Studies have shown that the maximum vertical temperature gradient of bridge structure in the sunshine generally occurs in summer [24, 25]. In the present study, the temperature field of the steel box girder in the summer of 2018 is calculated to obtain the most disadvantageous temperature distribution of the steel box girder. The results indicate that the temperature differences along the bridge and along the thickness of steel plate are small, and the transverse temperature differences

with symmetrical distribution are less than 2°C, which can also be neglected.

In fact, the statistical results show that the maximum vertical temperature difference and the maximum vertical temperature gradient occur at different times, and the maximum vertical temperature difference generally appears at around 2:00 pm, while the maximum temperature gradient occurs around 5:00 pm. The comparison of the top and bottom temperatures of the pavement from 11th to 15th of August is depicted in Figure 8. As pictured in the figure, the time of daily maximum temperature at the bottom of pavement lags behind 2 or 3 hours compared with that of pavement surface. The reason for the temperature hysteresis is that the temperature of pavement surface will gradually decrease with the decline of radiation and air temperature after 2:00 pm, while asphalt pavement has a “thermal insulation effect” on the bottom of pavement of the box girder.

Further, the comparisons among the maximum vertical temperature difference, the maximum vertical temperature gradient, and the maximum vertical temperature gradient specified in the code is shown in Figure 9, which reveals that the temperature decreases fastest in the pavement, followed by the top plate and the web. Besides, the calculated maximum gradient in the bottom of pavement exceeds the gradient imposed in the code. Thus, it is necessary to analyze the temperature distribution of steel box girder under the extreme weather conditions.

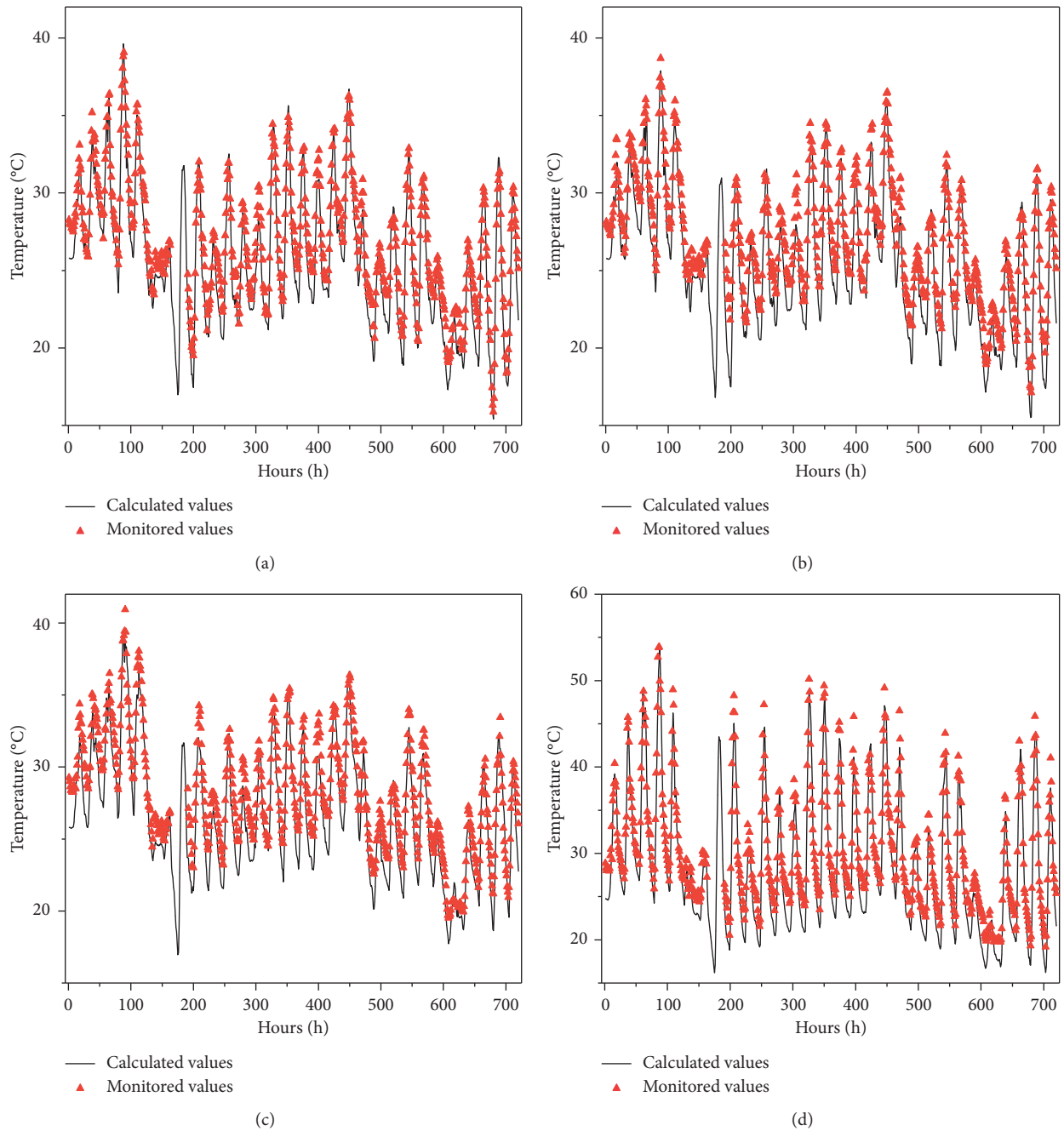


FIGURE 7: Comparisons of variation of temperature between calculated and monitored values of typical measuring points in September. (a) Flange measuring point T1. (b) Web measuring point T3. (c) Bottom measuring point T10. (d) Bridge deck measuring point IT1.

#### 4. Analysis of Temperature Field of Steel Box Girder under the Extreme Weather Conditions

**4.1. Sensitivity Analysis of Parameters.** Since the design reference period of the bridge structure is 100 years according to the design code, the extreme weather conditions should also be considered for a 100-year recurrence period. Thus, in order to obtain the temperature distribution of steel box girder under the extreme weather conditions during 100-year return period, the sensitivity of main

meteorological parameters affecting temperature distribution is investigated with the help of the proposed model.

In general, solar radiation, air temperature, and wind speed are considered as the main meteorological parameters [26], which vary from place to place depending on different exposure conditions. Hence, it is worthwhile to implement the sensitivity studies on the influences of the above three meteorological factors on the maximum vertical temperature gradient through employing the control variable method, which is to control a meteorological parameter to increase or decrease by 10% orderly based on

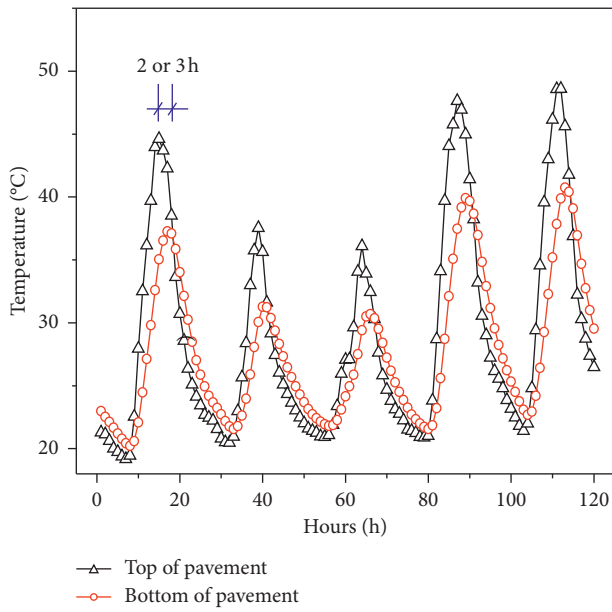


FIGURE 8: Comparison of variation of temperature between the top and bottom of pavement.

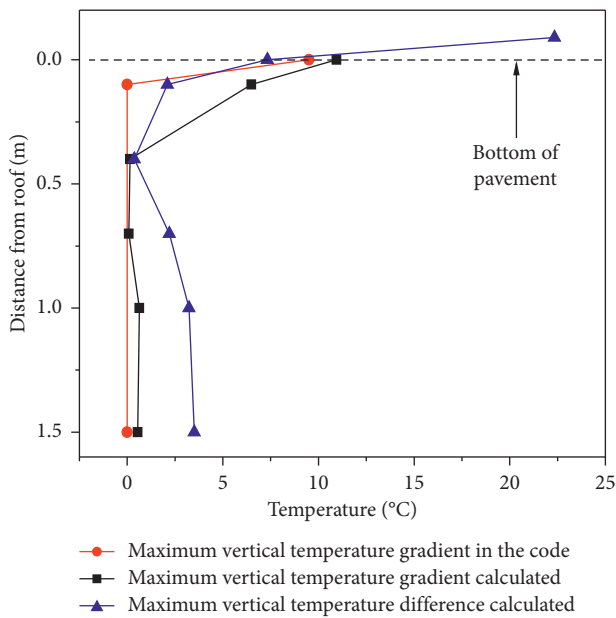


FIGURE 9: Comparisons of vertical temperature differences.

the measured values recorded at weather station, while the other two parameters remain fixed at the same time. The analytical results are shown in Figure 10. It can be evidently found that solar radiation has the most significant influence on the maximum vertical temperature gradient, followed by air temperature and wind speed. Moreover, air temperature and solar radiation are positively correlated with the maximum vertical temperature gradient, while wind speed is negatively correlated with it. What is more, the maximum vertical temperature gradient of steel box girder increases (or decreases) by about 30% and 10%, respectively, with the increase (or decrease) of solar radiation and

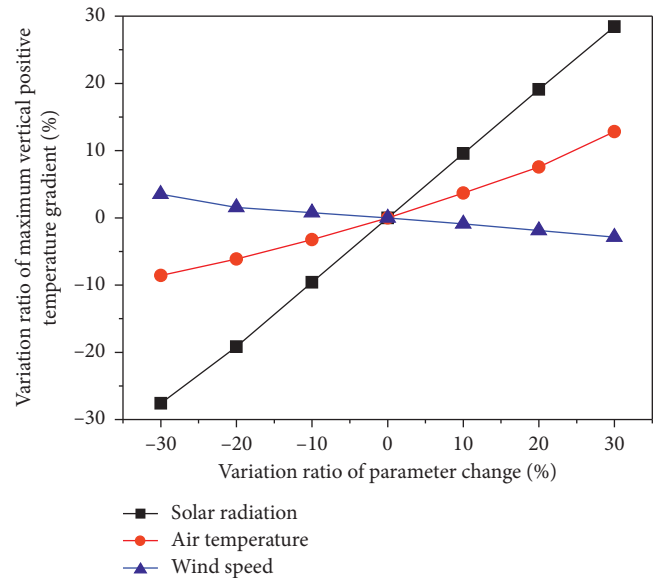


FIGURE 10: Sensitivity curves of the parameters.

air temperature by 30%, while the maximum temperature gradient of steel box girder decreases (or increases) by about 4% with the increase (or decrease) of wind speed by 30%.

**4.2. Determination of the Extreme Representative Values of Meteorological Parameters.** Figure 10 shows that the influence of wind speed on the maximum vertical temperature gradient is the smallest among the three parameters. Generally, the variations of wind speed have no obvious regularity and the discreteness of values is large. To facilitate the selection of values, the hourly average wind speed in Wuhan from July to September, 2018, is taken as the hourly representative values of the extreme wind speed. The Design Code for Heating Ventilation and Air Conditioning for Industrial Buildings [27] has a regulation on hourly extreme solar radiation in Wuhan, and the representative values in the code are conservative. Thus, the hourly representative values of the extreme solar radiation in Wuhan (30.07 north latitude and level 3 atmospheric transparency) can be determined.

Due to the variations of air temperature and the fact that the influence of temperature change on the maximum vertical temperature gradient is significant, the statistical method is applied herein for analysis purpose. By collecting the air temperature data of Wuhan from 2011 to 2018, it is verified that the daily maximum temperature of summer approximately obeys the Gumbel distribution with parameters (0.33, 29.39), of which the density function and the distribution curve are shown in equation (3) and Figure 11(a), respectively. The maximum daily air temperature difference approximately obeys the normal distribution with parameters (8.705, 3.08) by the chi-square test, of which the density function and the distribution curve are shown in equation (4) and Figure 11(b), respectively:

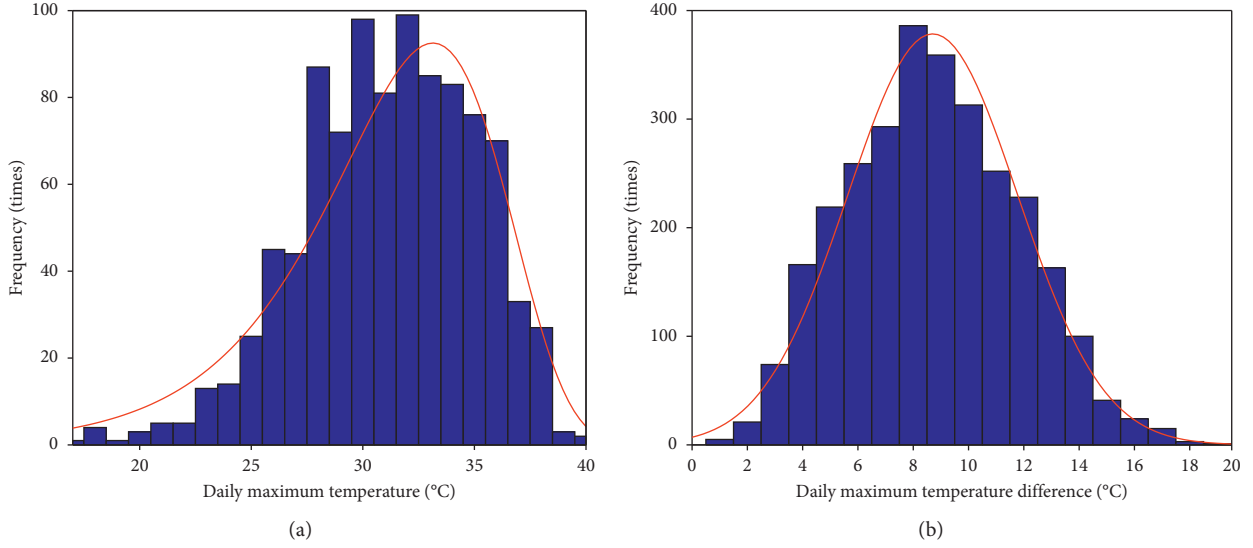


FIGURE 11: Probability distribution curve. (a) Gumbel distribution. (b) Normal distribution.

$$F(x) = e^{-e^{-0.33(x-29.39)}}, \quad (3)$$

$$F(x) = \frac{1}{\sqrt{2\pi}\sigma} \int_{-\infty}^x e^{-(x-\sigma)^2/2\sigma^2} dx. \quad (4)$$

Since the recurrence period of meteorological parameters is considered as 100 years, the relationship between the recurrence period and the guaranteed rate in exceeding probability is presented in equation (5). In the case of substituting the guaranteed rate of 99% when  $T_0 = 100$  into equation (5), the daily maximum temperature and the daily maximum temperature difference can thus be calculated through the probability distributions expressed in equations (3) and (4), which are 45°C and 16°C, respectively. According to the hourly temperature of Wuhan in the summer of 2018, the fitted temperature variation function is studied and shown in equation (6). By substituting the maximum and minimum air temperature in 100-year return period into equation (6), the hourly representative values of the extreme air temperature can be obtained easily:

$$P = 1 - \frac{1}{T_0}, \quad (5)$$

$$T = \begin{cases} \frac{T_{\max} + T_{\min}}{2} - \frac{T_{\max} - T_{\min}}{2} \sin\left(\frac{t+4}{16}\pi\right), & 0 \leq t \leq 5, \\ \frac{T_{\max} + T_{\min}}{2} - \frac{T_{\max} - T_{\min}}{2} \sin\left(\frac{t+2.2}{10.8}\pi\right), & 6 \leq t \leq 15, \\ \frac{T_{\max} + T_{\min}}{2} + \frac{T_{\max} - T_{\min}}{2} \sin\left(\frac{t-8.5}{11.8}\pi\right), & 16 \leq t \leq 23. \end{cases} \quad (6)$$

4.3. Analysis of Calculation Results under the Extreme Meteorological Conditions. The representative values of the

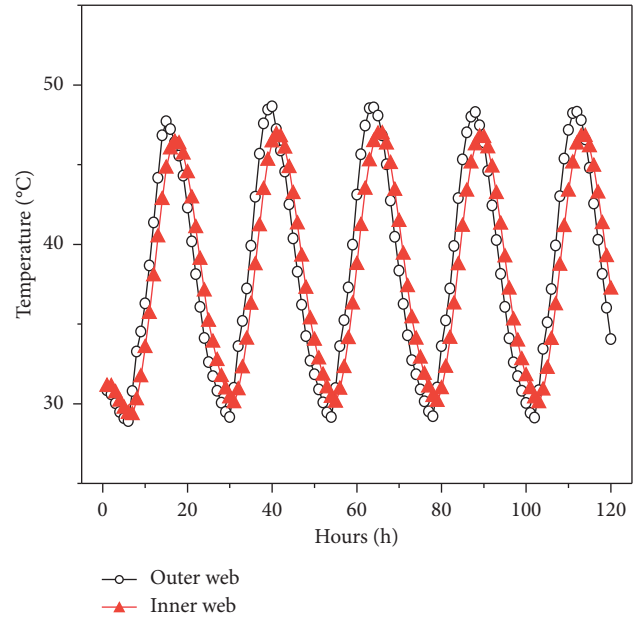


FIGURE 12: Comparison of variation of temperature between inner and outer webs.

extreme meteorological parameters obtained in the previous section are used as weather documents to calculate the temperature distribution of the steel box girder for 5 consecutive days. Figure 12 suggests that the time when the temperature of the inner web reaches its maxima and minima lags behind 2 hours than the outer web. Beyond that, the daily maximum temperature of the inner web is 2°C lower than that of the outer web approximately, and the daily minimum temperature is about 2°C higher than the outer web.

The maximum temperature gradient calculated is higher than the gradient specified in the code in Figure 13. Moreover, the cooling modes between the inner and outer

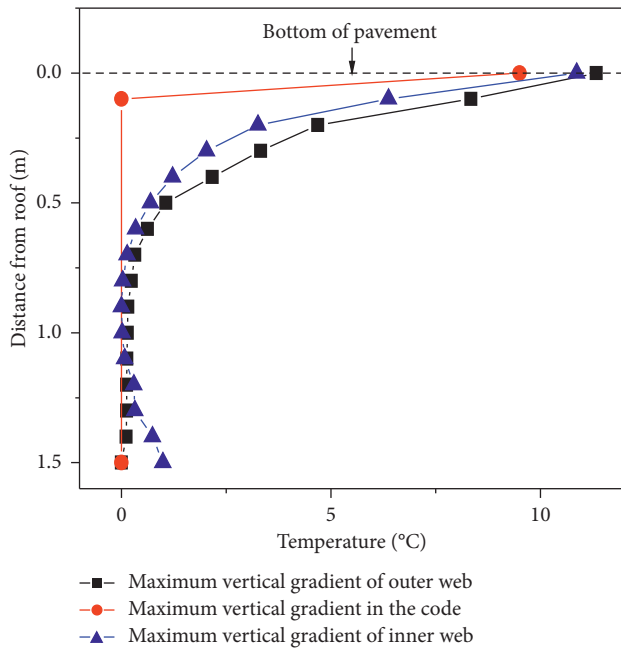


FIGURE 13: Distribution patterns of maximum vertical temperature gradient.

webs near the bottom plate are quite different (see Figure 13), which is the distinct “box-room effect” reflected during the heat conduction process in steel box girder [28]. Specifically, the “box-room effect” of the steel box girder is particularly embodied in the following four aspects: (1) the times when the inner and outer webs reach the daily maximum temperature are different; (2) the maximum daily temperatures of inner and outer web are different; (3) the maximum vertical temperature gradients in the top and bottom plates are higher than those in the existing standards; (4) the temperature variation patterns of the inner and outer webs are diverse.

As a result, the “box-room effect” makes the temperature distribution more complicated, which may inevitably lead to more severe stress concentration and structural safety risks of bridge structures. Consequently, this phenomenon should be adequately considered in case of analyzing the temperature effect of steel box girder in the sunshine to preferably ensure the safety of bridge structures during their service lives.

## 5. Conclusions

A spatial-temporal temperature field model of steel box girder of a 3-span continuous steel box girder in Wuhan is developed with the help of the software TAITHERM in this study. Moreover, the sunshine temperature field of the steel box girder is thoroughly scrutinized. Then, considering the representative values of the extreme meteorological parameters during 100-year return period in Wuhan as the thermal boundary conditions, the temperature distribution of steel box girder under such environmental conditions is studied in detail. The conclusions drawn from the study can be summarized as follows:

- (1) The calculated temperature values of pavement and girder are in good agreement with the monitoring values, which shows that the proposed temperature field model of steel box girder is of great effectiveness. Thus, it can be widely used for accurate analysis of temperature field of steel box girder.
- (2) The transverse temperature differences of the top and bottom plates of the steel box girder and the temperature differences along the longitudinal direction of bridge and along the thickness of the steel plates are very small, which can thus be neglected, while, due to the thermal insulation effect of pavement on the top plate of the steel box girder, the time when the bottom of pavement reaches the maximum daily temperature lags behind 2 or 3 hours than the surface of pavement.
- (3) Solar radiation has the most significant influence on the maximum vertical temperature gradient of the steel box girder, followed by air temperature and wind speed. In addition, the maximum vertical temperature gradient is positively correlated with solar radiation and air temperature, while it is negatively correlated with wind speed.
- (4) According to the collected air temperature of Wuhan, the hourly temperature variation function and the hourly representative values of the extreme air temperature during 100-year return period can be obtained by means of the statistical method.
- (5) Under the extreme weather conditions, the time when the temperature of the inner web reaches its maximum and minimum is about 2 hours behind the outer web, and the maximum (or minimum) daily temperature of the inner web is lower (or higher) than the outer web by about 2°C. Moreover, the maximum vertical temperature gradient is larger than design code. Thus, the actual meteorological conditions at the bridge site and the “box-room effect” of the steel box are of nonnegligible significance in engineering practices.

In summary, the temperature distribution proposed in this paper is applicable to establish the temperature field of steel box girders in Wuhan area and also other areas with similar latitudes and climate conditions. In fact, the suggested approach is of great universality in engineering applications. As for various types of bridges in different regions, the spatial-temporal model of thermal field can be established according to the measured meteorological data at the bridges site, the geometric shapes, and material properties of the specific bridge bridges. Moreover, the calculated temperature values can provide an effective and advantageous reference for studying the thermal behaviors in the future.

## Data Availability

The data used to support the findings of this study are available from the corresponding author upon request.

## Conflicts of Interest

The authors declare that there are no conflicts of interest regarding the publication of this paper.

## Acknowledgments

The research in this paper was supported by (1) the Graduate Education Innovation Fund Project of Wuhan Institute of Technology (Grant no. CX2018037), (2) Wuhan Institute of Technology Science Found (Grant no. K201734), (3) the National Natural Science Foundation of China (Grants nos. 51708429, 51708428, and 51609181), and (4) the Opening Project Foundation (Grant no. 2017-04-GF) of State Key Laboratory for Health and Safety of Bridge Structures.

## References

- [1] J. F. Wang, Z. Y. Xu, X. L. Fan, and J. P. Lin, "Thermal effects on curved steel box girder bridges and their countermeasures," *Journal of Performance of Constructed Facilities*, vol. 31, no. 2, Article ID 04016091, 2017.
- [2] M. Tong, L. G. Tham, F. T. K. Au, and P. K. K. Lee, "Numerical modelling for temperature distribution in steel bridges," *Computers & Structures*, vol. 79, no. 6, pp. 583–593, 2001.
- [3] K. Mei, S. Sun, G. Jin, and Y. Sun, "Static and dynamic mechanical properties of long-span cable-stayed bridges using CFRP cables," *Advances in Civil Engineering*, vol. 2017, Article ID 6198296, 11 pages, 2017.
- [4] D. Zheng, Z.-D. Qian, D.-X. Liu, X.-F. Zhang, and Y. Liu, "Thermal field characteristics of reinforced concrete box girder during high-temperature asphalt pavement paving," *Transportation Research Record: Journal of the Transportation Research Board*, vol. 2672, no. 41, pp. 56–64, 2018.
- [5] H. Liu, Z. Chen, and T. Zhou, "Theoretical and experimental study on the temperature distribution of H-shaped steel members under solar radiation," *Applied Thermal Engineering*, vol. 37, pp. 329–335, 2012.
- [6] Z. Yu, Y. Xie, and X. Tian, "Research on mechanical performance of CRTS III plate-type ballastless track structure under temperature load based on probability statistics," *Advances in Civil Engineering*, vol. 2019, Article ID 2975274, 16 pages, 2019.
- [7] W. Zuk, "Thermal and shrinkage stresses in composite bridges," *Journal of the American Concrete Institute*, vol. 58, no. 3, pp. 327–340, 1961.
- [8] F. Au, L. Tham, M. Tong et al., "Temperature monitoring of steel bridges," in *Proceedings of SPIE—The International Society for Optical Engineering*, vol. 4337, pp. 282–291, San Diego, CA, USA, August 2001.
- [9] M. M. Elbadry and A. Ghali, "Temperature variations in concrete bridges," *Journal of Structural Engineering*, vol. 109, no. 10, pp. 2355–2374, 1983.
- [10] B. Gu, Z.-J. Chen, and X.-D. Chen, "Temperature gradients in concrete box girder bridge under effect of cold wave," *Journal of Central South University*, vol. 21, no. 3, pp. 1227–1241, 2014.
- [11] S.-H. Kim, K.-I. Cho, J.-H. Won, and J.-H. Kim, "A study on thermal behaviour of curved steel box girder bridges considering solar radiation," *Archives of Civil and Mechanical Engineering*, vol. 9, no. 3, pp. 59–76, 2009.
- [12] Q. Meng and J. Zhu, "Fine temperature effect analysis-based time-varying dynamic properties evaluation of long-span suspension bridges in natural environments," *Journal of Bridge Engineering*, vol. 23, no. 10, Article ID 04018075, 2018.
- [13] J. Zhu and Q. Meng, "Effective and fine analysis for temperature effect of bridges in natural environments," *Journal of Bridge Engineering*, vol. 22, no. 6, Article ID 04017017, 2017.
- [14] J.-H. Lee and I. Kalkan, "Analysis of thermal environmental effects on precast, prestressed concrete bridge girders: temperature differentials and thermal deformations," *Advances in Structural Engineering*, vol. 15, no. 3, pp. 447–459, 2012.
- [15] J. Liu, Y. Liu, and G. Zhang, "Experimental analysis of temperature gradient patterns of concrete-filled steel tubular members," *Journal of Bridge Engineering*, vol. 24, no. 11, Article ID 04019109, 2019.
- [16] Y. Ding, G. Zhou, A. Li, and G. Wang, "Thermal field characteristic analysis of steel box girder based on long-term measurement data," *International Journal of Steel Structures*, vol. 12, no. 2, pp. 219–232, 2012.
- [17] Y.-L. Ding and G.-X. Wang, "Estimating extreme temperature differences in steel box girder using long-term measurement data," *Journal of Central South University*, vol. 20, no. 9, pp. 2537–2545, 2013.
- [18] M. J. S. Hirst, "Thermal loading of concrete bridges," *Canadian Journal of Civil Engineering*, vol. 11, no. 3, pp. 423–429, 1984.
- [19] D. Ho and C. H. Liu, "Extreme thermal loadings in highway bridges," *Journal of Structural Engineering*, vol. 115, no. 7, pp. 1681–1696, 1989.
- [20] J.-M. Lucas, M. Virlogeux, and C. Louis, "Temperature in the box girder of the normandy bridge," *Structural Engineering International*, vol. 15, no. 3, pp. 156–165, 2005.
- [21] JTG D60-2015, *General Specification for Design of Highway Bridges and Culverts*, Ministry of communications of the People's Republic of China, Beijing, China, 2015.
- [22] M. Tong, L. G. Tham, and F. T. K. Au, "Extreme thermal loading on steel bridges in tropical region," *Journal of Bridge Engineering*, vol. 7, no. 6, pp. 357–366, 2002.
- [23] L. Zhou, Y. Xia, J. M. W. Brownjohn, and K. Y. Koo, "Temperature analysis of a long-span suspension bridge based on field monitoring and numerical simulation," *Journal of Bridge Engineering*, vol. 21, no. 1, Article ID 04015027, 2016.
- [24] J.-H. Lee, "Investigation of extreme environmental conditions and design thermal gradients during construction for prestressed concrete bridge girders," *Journal of Bridge Engineering*, vol. 17, no. 3, pp. 547–556, 2012.
- [25] S. R. Abid, N. Tayşi, and M. Özakça, "Experimental analysis of temperature gradients in concrete box-girders," *Construction and Building Materials*, vol. 106, pp. 523–532, 2016.
- [26] C. Jing and J. Zhang, "Prediction model for asphalt pavement temperature in high-temperature season in Beijing," *Advances in Civil Engineering*, vol. 2018, Article ID 1867952, 11 pages, 2018.
- [27] GB50019-2015, *Design Code for Heating Ventilation and Air Conditioning for Industrial Buildings*, Ministry of housing and urban-rural development of the People's Republic of China, Beijing, China, 2015.
- [28] C. Miao and C. Shi, "Temperature gradient and its effect on flat steel box girder of long-span suspension bridge," *Science China Technological Sciences*, vol. 56, no. 8, pp. 1929–1939, 2013.